Functional Role of "N" (Nucleotide) and "P" (Phosphorylation) Domain Interactions in the Sarcoplasmic Reticulum (SERCA) ATPase†

Suming Hua, Hailun Ma, David Lewis, and Giuseppe Inesi*

Department of Biochemistry and Molecular Biology, University of Maryland School of Medicine, Baltimore, Maryland 21201

Chikashi Toyoshima

Institute of Molecular and Cellular Biosciences, University of Tokyo, Bunkyo-ku, Tokyo 113, Japan

Received August 14, 2001; Revised Manuscript Received December 17, 2001

ABSTRACT: Experimental perturbations of the nucleotide site in the N domain of the SR Ca^{2+} ATPase were produced by chemical derivatization of Lys492 or/and Lys515, mutation of Arg560 to Ala, or addition of inactive nucleotide analogue (TNP-AMP). Selective labeling of either Lys492 or Lys515 produces strong inhibition of ATPase activity and phosphoenzyme intermediate formation by utilization of ATP, while AcP utilization and reverse ATPase phosphorylation by Pi are much less affected. Cross-linking of the two residues with DIDS, however, drastically inhibits utilization of both ATP and AcP, as well as of formation of phosphoenzyme intermediate by utilization of ATP, or reverse phosphorylation by Pi. Mutation of Arg560 to Ala produces strong inhibition of ATPase activity and enzyme phosphorylation by ATP but has a much lower effect on enzyme phosphorylation by Pi. TNP-AMP increases the ATPase activity at low concentrations (0.1−0.3 μM), but inhibits ATP, AcP, and Pi utilization at higher concentration (1−10 μM). Cross-linking with DIDS and TNP-AMP binding inhibits formation of the transition state analogue with orthovanadate. It is concluded that in addition to the binding pocket delimited by Lys 492 and Lys515, Arg560 sustains an important and direct role in nucleotide substrate stabilization. Furthermore, the effects of DIDS and TNP-AMP suggest that approximation of N (nucleotide) and P (phosphorylation) domains is required not only for delivery of nucleotide substrate, but also to favor enzyme phosphorylation by nucleotide and nonnucleotide substrates, in the presence and in the absence of Ca^{2+}. Domain separation is then enhanced by secondary nucleotide binding to the phosphoenzyme, thereby favoring its hydrolytic cleavage.

The SR Ca^{2+} ATPase is a member of an important family of transport ATPases (SERCA)[1] that are required for cellular homeostasis and Ca^{2+} signaling functions. The membrane bound ATPase can be isolated in association with microsomal vesicles and provides a favorable system for functional and structural studies. Its catalytic and transport cycle begins with high affinity binding of medium Ca^{2+}, followed by utilization of ATP to form a phosphorylated enzyme intermediate, dissociation of the bound Ca^{2+} in the lumen of the vesicles, and hydrolytic cleavage of Pi:

$$E + 2Ca^{2+}_{out} \leftrightarrow E_1{\cdot}Ca_2 \quad (1)$$

$$E_1{\cdot}Ca_2 + ATP \leftrightarrow ATP{\cdot}E_1{\cdot}Ca_2 \quad (2)$$

$$ATP{\cdot}E_1{\cdot}Ca_2 \leftrightarrow E_1{-}P{\cdot}Ca_2 + ADP \quad (3)$$

$$E_1{-}P{\cdot}Ca_2 \leftrightarrow E_2{-}P{\cdot}Ca_2 \quad (4)$$

$$E_2{-}P{\cdot}Ca_2 \leftrightarrow E_2{-}P + Ca^{2+}_{in} \quad (5)$$

$$E_2{-}P \leftrightarrow E + Pi \quad (6)$$

It is generally accepted that E_1 and E_2 correspond to enzyme conformations of high and low affinity for Ca^{2+}, and opposite orientation of the Ca^{2+} sites. The E_1 state is induced by Ca^{2+} binding, and the E_2 state by enzyme phosphorylation with ATP. Thereby, the free energy of ATP is utilized to form a transmembrane Ca^{2+} gradient.

The crystal structure of the SR ATPase in the Ca^{2+} bound conformation was recently described by Toyoshima et al. (*1*). An important feature of the Ca^{2+} bound conformation is a wide separation of the nucleotide ("N") binding and the phosphorylation ("P") domains, suggesting that approximation of the two domains must occur to allow utilization of nucleotide substrate at the phosphorylation site. In fact, the

†This work was supported by National Institutes of Health Program Project HL27867, the Human Frontier Science Program, and grants-in-aid for scientific research and for international scientific research from the Ministry of Education, Science, Sports and Culture of Japan.

* Corresponding author. Telephone: 410-706-3220. Fax: 410-706-8297. E-mail: ginesi@umaryland.edu.

[1] Abbreviations: AcP, acetyl phosphate; AMP−PNP, 5′-adenylylimidodiphosphate; DIDS, 4,4′-diisothiocyanatostilbene 2,2′-disulfonic acid; EGTA, ethylene glycol-bis(aminoethyl ether)-*N*,*N*,*N*′,*N*′-tetraacetic acid; FITC, fluorescein-5-isothiocyanate; LDH, L-lactic dehydrogenase; MOPS, 4-morpholinepropanesulfonic acid; NADH, beta-nicotinamide adenine dinucleotide; PEP, phospho(enol)pyruvate; PK, pyruvate kinase; PYP, pyridoxal 5′-phosphate; SERCA, sarco-endoplasmic reticulum Ca^{2+} ATPases; SR, sarcoplasmic reticulum; TNP-AMP, 2′(or 3′)-*O*-(trinitrophenyl)adenosine 5′-monophosphate; TRIS, tris(hydroxymethyl)aminomethane; A, N, and P domains, small cytosolic, nucleotide binding, and phosphorylation domains, respectively.

10.1021/bi015684h CCC: $22.00
Published on Web 01/24/2002

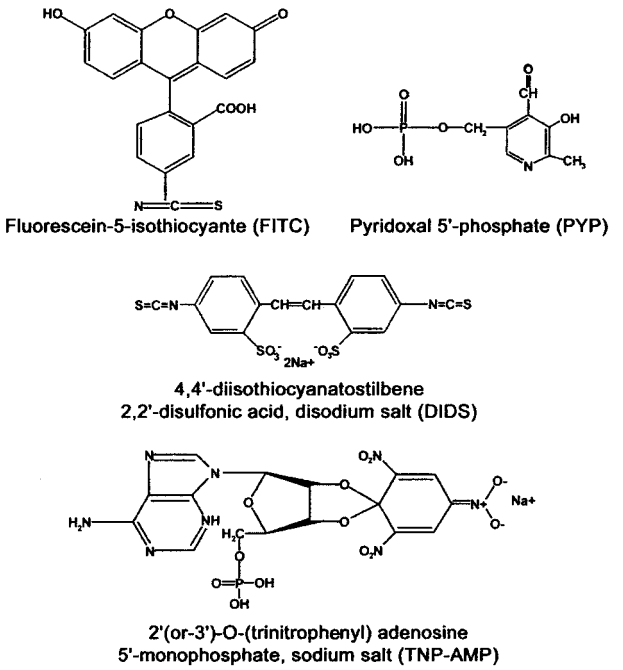

FIGURE 1: Structures of pyridoxal 5′-phosphate (PYP), fluorescein-5-isothiocyanate (FITC), 4,4′-diisothiocyanatostilbene-2,2′-disulfonic acid (DIDS), and 2′(or 3′)-*O*-(trinitrophenyl) adenosine 5′-monophosphate (TNP-AMP).

N and P domains (as well as an additional and smaller "A" domain) appear much closer to each other in maps derived from electron microscopy of tubular crystals obtained in the absence of Ca^{2+} and in the presence of decavanadate (*2*, *3*). It is noteworthy that the Ca^{2+} binding residues (*4*) are located within the transmembrane region, separated by a distance of more than 50 Å from phosphorylation and nucleotide binding sites (*1*, *5*).

Another important feature of the published structure (*1*) is the identification of the TNP-AMP binding site within the N domain. The TNP-AMP adenine moiety lies within a pocket delimited by Lys 492 and Lys515, with Arg560 in close proximity. Lys492 and Lys515 can be derivatized selectively with FITC (*6*, *7*) or PYP (*8*, *9*), respectively, or cross-linked with DIDS (*10*, *11*). We then performed a series of experiments to characterize in detail the functional effects of TNP-nucleotide, Lys492, and Lys515 derivatization, or mutation of Arg560, to discover whether experimental perturbations of the N domain interfere with ATPase reactions that occur in the P domain. The aim was to define the role of the N domain in delivering the substrate and to explore whether interactions of P and N domains are an integral part of a global catalytic mechanism.

MATERIALS AND METHODS

TNP-AMP, TNP-ATP, FITC, and DIDS were purchased from Molecular Probes. AMP−PNP, PYP, and other reagents were purchased from SIGMA. SR vesicles were obtained by homogenization and differential centrifugation of rabbit skeletal muscle, as described by Eletr and Inesi (*12*). The structures of FITC, PYP, DIDS, and TNP-AMP are given in Figure 1.

Derivatization of Lys492 with PYP was produced according to Yamagata et al. (*9*) by incubating SR vesicles (2 mg of protein/mL) with 2 mM PYP in a medium containing 50 mM MOPS, pH 7, 5 mM $MgCl_2$, 0.1 M KCl, 1 mM EGTA, and 0.1 M sucrose, protected with aluminum foil, at 25 °C for 8 min. The reaction was quenched by adding $NaBH_4$ to 3 mM final concentration. The reacted vesicles were sedimented by centrifugation and washed twice with 50 mM MOPS, pH 7, 0.1 M KCl, 5 mM $MgCl_2$, 0.5 mM $CaCl_2$, 0.4 mM EGTA, and 0.1 M sucrose. Alternatively, the reacted SR vesicles were separated from the reaction mixture on a gel filtration column.

Derivatization of Lys515 with FITC was produced according to Pick (*13*) by incubating SR vesicles (1 mg/mL) with 15 μM FITC in a medium containing 10 mM TRIS, pH 9.2, 0.1 M KCl, 0.3 M sucrose, and 0.1 mM EGTA, protected with aluminum foil, at 22 °C for 10 min. The reaction mixture was then placed on a column for separation of the reacted vesicles by gel filtration.

Cross-linking of Lys492 and Lys515 with DIDS was obtained according to Hua and Inesi (*10*), as adapted from Gatto et al. (*11*). SR vesicles (1 mg of protein/mL) were reacted with 20 μM DIDS in a medium containing 10 mM TRIS, pH 9.2, 0.1 M KCl, 0.3 M sucrose, and 0.1 mM EGTA, protected with aluminum foil, at 22 °C for 1 h. The reaction mixture was then placed on a column for separation of the reacted vesicles by gel filtration.

Recombinant Ca^{2+} ATPase protein was obtained from COS-1 cells following infection with adenovirus vectors carrying WT or mutated SERCA-1 cDNA. Cell cultures, recombinant cDNA procedures, harvesting of cells and preparation of microsomal fractions were carried out as previously described (*14*).

ATPase activity was measured either by determination of Pi by a colorimetric method (*15*), or by spectrophotometric determination of NADH oxidation coupled to an ATP regenerating system. AcPase activity was measured by determination of residual AcP as described by Lippman and Tuttle (*16*). Both ATPase and AcP velocities were derived from linear plots of several time points. The reaction mixtures are given in the legends for the figures.

Phosphoenzyme formation by utilization of ATP was obtained under steady-state conditions by reacting SR vesicles with [^{32}P]ATP, and measuring the incorporation of radioactivity in the protein. Following 10 s incubation at 2 °C, the reaction was quenched with 1 M PCA, and the quenched protein was washed three times by centrifugation and suspension in 0.125 M PCA, and once with cold water. The washed sediment was then dissolved and subjected to electrophoresis (*17*). Reaction conditions are given in the legends to the figures.

Phosphoenzyme formation by utilization of Pi was obtained under equilibrium conditions by reacting SR vesicles with [^{32}P]Pi, and measuring the incorporation of radioactivity in the protein. Following 5 min incubation at 25 °C, the reaction was quenched by addition of 1 M PCA/2 mM Pi, and the quenched protein was washed with 0.125 M PCA/1 mM Pi and cold water as described above. When low quantities of protein were used for the phosphorylation reaction, additional quenched SR protein was added as a carrier before washing. A small aliquot of the washed protein was used to quantitate recovery, and a larger aliquot was processed for radioactivity counting. Alternative, the washed protein was subjected to electrophoresis (*17*) and phospho-

imaging. Reaction conditions are given in the legends to the figures.

TNP-AMP binding to SR vesicles was measured by fluorescence spectroscopy, with 420 nm excitation wavelength and 540 nm emission wavelength. The composition of media is given in the legends to the figures.

Orthovanadate-dependent photooxidation of ATPase was carried out at pH 8.6, in a reaction mixture containing 50 mM Tris-Cl buffer, 100 mM KCl, 5 mM $MgCl_2$, 0.1 mM $CaCl_2$, 1 mM vanadate, and 1.0 mg of microsomal protein/mL. After 30 min preincubation, the mixture was illuminated for 15 min with long wavelength UV light. The protein was then subjected to electrophoretic analysis by the method of Weber and Osborn (*17*).

ATPase digestion with proteinase K was carried out at pH 8.0, in a reaction mixture containing 50 mM MOPS buffer, 50 mM NaCl, 5 mM $MgCl_2$, 2 mM EGTA, and 0.3 mg of microsomal protein/mL with 0.01 mg/mL proteinase K. The mixture was incubated at 25 °C, for 40 min, and stopped by addition of ice-cold trichloroacetic acid to 2.5% (w/v). The protein was then subjected to electrophoretic analysis by the method of Laemmli (*18*).

Electrophoresis (*17*, *18*) was carried out by placing 10−30 μg of protein in each well of 7.5% polyacrylamide minigels, run at a constant current of 75−100 mA for 1 h at 15 °C. For electrophoresis of phosphorylated protein, the pH of the running buffer was adjusted to 6.3, and lithium dodecyl sulfate (instead of SDS) was used to avoid precipitation. The gels were stained with Coomassie Blue, and/or subjected to autoradiography and quantitative phosphoimaging.

Error bars in all graphs represent standard deviations derived from three to seven measurements.

RESULTS

Functional Effects of Lys492 and Lys515 Derivatization or Cross-Linking. It is known that the Ca^{2+} ATPase dependence on the ATP concentration is biphasic (*19*). A first rise of the ATP concentration dependence curve is observed (Figure 2) within the 1−10 μM range, due to ATP interaction with the catalytic site, and a second rise within the 0.1−1.0 mM range, due to ATP occupancy of a lower affinity activating site.

Derivatization of Lys492 with PYP (*9*), derivatization of Lys515 with FITC (*6*), or cross-linking of Lys492 and Lys515 with DIDS (*10*), produce strong ATPase inhibition, throughout a wide range of ATP concentrations (Figure 2). This is consistent with previous studies showing the same pattern of inhibition following derivatization of homologous residues in the Na^+,K^+ ATPase with DIDS (*11*, *20*).

To characterize with greater detail the mechanism of inhibition, we then measured formation of phosphorylated intermediate by utilization of ATP in the presence of Ca^{2+} (reaction 3 in the sequence given in the introduction). Phosphoenzyme formation occurs rapidly upon addition of ATP, reaching steady-state levels within 10 s at 2 °C (*21*). It is shown in Figure 3 that derivatization of Lys492 or/and Lys515 produces strong inhibition of phosphoenzyme formation by utilization of ATP. We found that maximal levels of phosphoenzyme are obtained with control SR in the presence of 2 μM ATP (Figure 3), but no significant signals is obtained

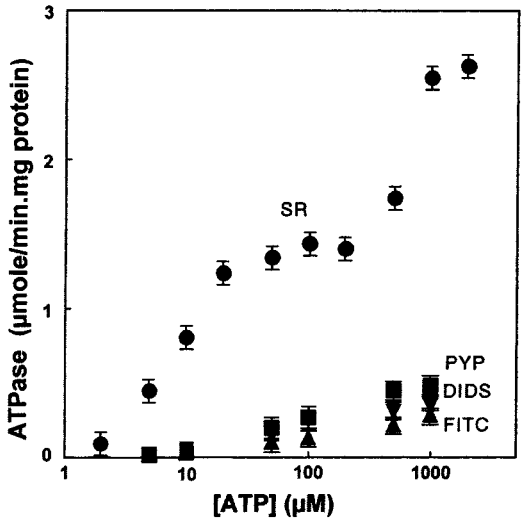

FIGURE 2: Effect of enzyme derivatization with PYP (■), FITC (▲), and DIDS (▼) on ATPase activity at various ATP concentrations. SR control: ●. ATPase activity was measured at 22 °C, in the presence of 20 mM MOPS, pH 7.0, 80 mM KCl, 5 mM $MgCl_2$, 5 μg of SR protein/mL, 50 μM $CaCl_2$, 3 μM A23187 (calcium ionophore), 2 mM PEP, 25 U PK/mL, 25 U LDH/mL, 0.15 mM LADH, and various ATP concentrations. The activity was recorded spectrophotometrically, and the velocities were derived from linear plots.

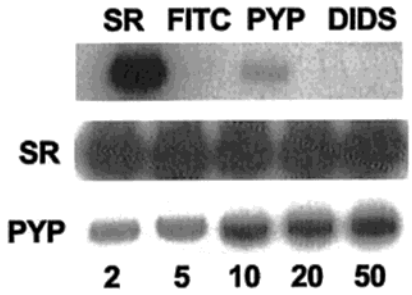

FIGURE 3: Effect of enzyme derivatization with PYP, FITC, and DIDS on phosphoenzyme intermediate formation by utilization of ATP. Reaction mixture: 20 mM MOPS, pH 7.0, 80 mM KCl, 5 mM $MgCl_2$, 10 μM $CaCl_2$, 10 μg of protein/mL sample and 2 μM (^{32}P)ATP (upper lane). The ATP concentration was varied as indicated (μM) in the lower two lanes. Following incubation for 10 s at 2 °C, the protein was quenched, washed, and processed for electrophoresis and autoradiography (see Methods).

with FITC or DIDS derivatized enzyme within the 2−50 μM range of ATP. On the other hand, the phosphoenzyme level of PYP derivatized enzyme increases significantly as the ATP concentration is raised (Figure 3).

The location of Lys492 and Lys515 within the adenosine binding pocket (*1*) suggests that the inhibition of ATP utilization observed in our experiments may be simply due to interference with ATP binding. Nevertheless, we extended our experimentation to test whether formation of phosphoenzyme by utilization of Pi (*22*, *23*) in the absence of Ca^{2+} (reversal of reaction 6 in the sequence given in the introduction) was also affected. We found that selective derivatization of Lys492 with PYP, or of Lys515 with FITC does not affect the Pi reaction (Figure 4). On the other hand, cross-linking Lys492 and Lys515 with DIDS in the N domain, produced total inhibition of the Pi reaction in the P domain.

We then proceeded to test the effect of derivatization on the ATPase utilization of AcP, a nonnucleotide pseudosubstrate (*24*−*26*). Ca^{2+} dependent AcP utilization is coupled

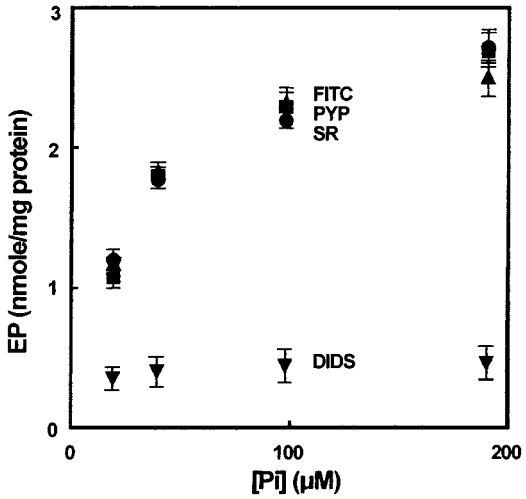

FIGURE 4: Effects of enzyme derivatization with PYP (■), FITC (▲), and DIDS (▼) on phosphoenzyme intermediate formation by utilization of Pi. SR control: ●. Enzyme phosphorylation with Pi was measured following equilibration at 25 °C for 10 min. The reaction mixture contained 50 mM MES, pH 6.2, 10 mM $MgCl_2$, 2 mM EGTA, 20% (v/v) Me_2SO, 30 μg of SR protein/mL, and (^{32}P)Pi as indicated.

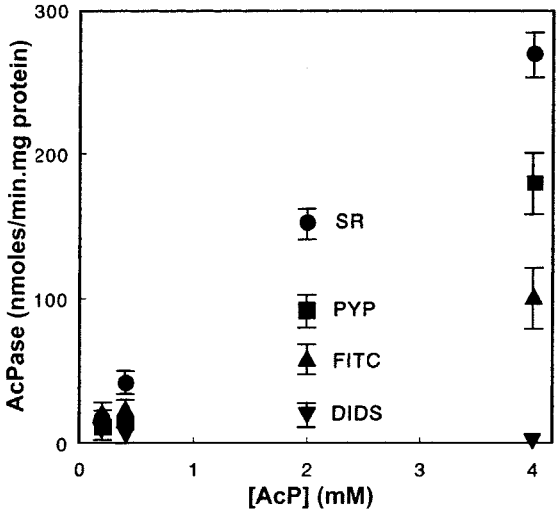

FIGURE 5: Effects of enzyme derivatization with PYP (■), FITC (▲), and DIDS (▼) on Ca^{2+} dependent AcPase activity, at various AcP concentrations. SR control: ●. AcPase activity was measured at 37 °C, in a medium containing 20 mM MOPS, pH 7.0, 80 mM KCl, 5 mM $MgCl_2$, 50 μg of SR protein/mL, and AcP as indicated, in the presence of 40 μM $CaCl_2$, or in the presence of 1 mM EGTA and no added calcium. Ca^{2+} dependent activity is the difference between that obtained in the presence of 40 μM $CaCl_2$ and that obtained in the presence of 1 mM EGTA and no added calcium. The velocities were derived from linear plots obtained from several time points.

to Ca^{2+} transport by a mechanism identical to that of ATP utilization (*27*, *28*), but inhibition by FITC is considerably less when AcP is used as a substrate instead of ATP (*6*, *13*, *28*). We found that while selective derivatization of Lys492 with PYP, or Lys515 with FITC produces only partial inhiibition, cross-linking of the two residues with DIDS produces total inhibition (Figure 5).

The experiments described above indicate that selective derivatization of Lys492 or Lys515 interferes with ATP and (to a lesser extent) AcP delivery to the catalytic site, but has no effect on enzyme phosphorylation by Pi. On the other hand, cross-linking of Lys492 and Lys515 by DIDS interferes

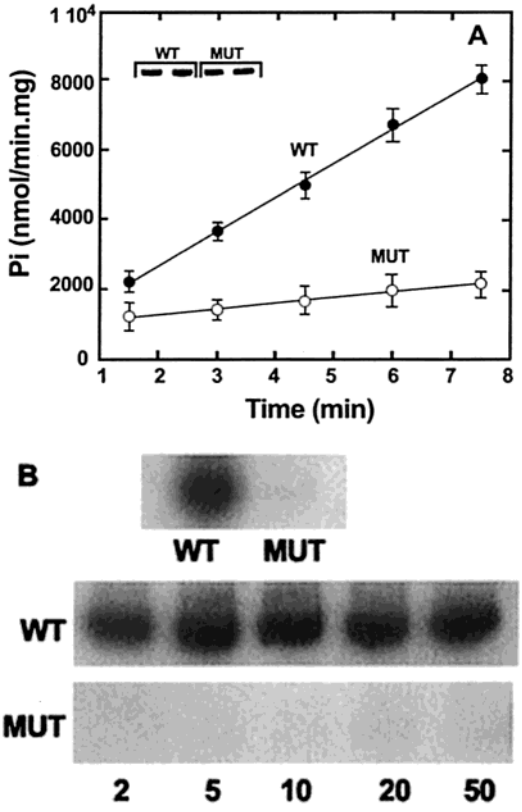

FIGURE 6: Functional characterization of the Arg560Ala mutant. The microsomal fractions of COS-1 cells infected with adenovirus vectors carrying WT or mutant SERCA1 cDNA, contained nearly identical levels of recombinant protein, as revealed by Western blots (inset in panel A). ATPase activity (A) was evaluated by measuring release of Pi in a medium containing 20 mM MOPS, pH 7.0, 80 mM KCl, 3 mM $MgCl_2$, 30 μg of microsomal protein/mL, 3 μM A23187 Ca^{2+} ionophore, 0.2 mM EGTA, 0.2 mM $CaCl_2$, and 3 mM ATP. Phosphoenzyme intermediate (B) formation by utilization of ATP was measured exactly as described for Figure 3, but with a higher protein concentration (50 μg/mL).

strongly with phosphorylation reaction at the catalytic site, independent of whether the substrate is ATP, AcP, or Pi, and of the presence or the absence of Ca^{2+}.

Functional Consequences of Arg560 Mutation to Ala. Considering the close proximity of Arg560 to the adenosine binding pocket of the N domain, we wondered whether the positive charge of that residue may contribute to substrate stabilization. We then mutated Arg560 to Ala, and compared the functional consequences of such mutation to those produced by lysine derivatization. We obtained expression of recombinant protein at identical levels in COS-1 cells infected with adenovirus vector carrying WT or mutant cDNA (Figure 6 A, inset). The Arg560 mutation produced strong inhibition of ATPase activity (Figure 6A), and of phosphoenzyme intermediate formation with ATP in the presence of Ca^{2+} (Figure 6B). The Arg560 mutation produced a much lower effect on reverse phosphoenzyme intermediate formation by the Pi reaction in the absence of Ca^{2+} (Figure 7).

Binding and Functional Effects of TNP-Nucleotide. Another group of experiments was performed to characterize the binding of the inactive nucleotide analogue TNP-AMP, and the effect of TNP-AMP occupancy of the nucleotide binding pocket on utilization of ATP, AcP, and Pi.

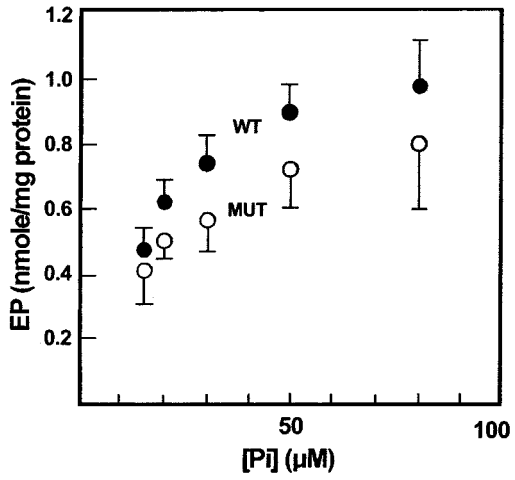

FIGURE 7: Effect of the Arg560 mutation to Ala on enzyme phosphorylation with Pi was obtained as described for Figure 4, but with a higher quantity (50−100 μg) of microsomal protein per sample. Parallel measurements were carried out counting total radioactivity of the quenched and washed protein, and by obtaining electrophoretic separation of the ATPase band, followed by phosphoimaging (see Methods). The lower phosphorylation levels, as compared to Figure 4, are due to the lower concentration of recombinant protein in the COS-1 cells microsomes, as compared to native SR vesicles.

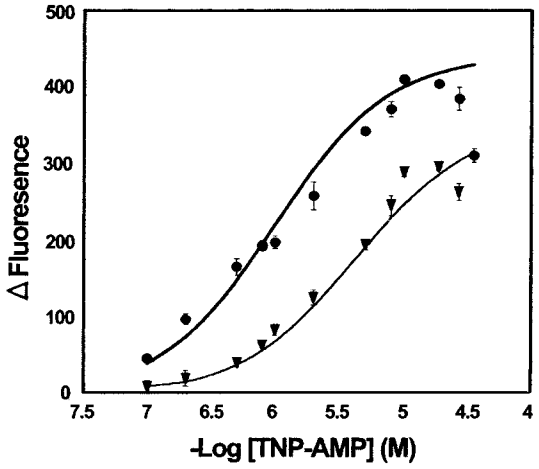

FIGURE 8: Effects of enzyme derivatization with DIDS on TNP-AMP binding to SR ATPase. SR control: ●. DIDS derivatized enzyme: ▼. Incremental quantities of TNP-AMP were added to a reaction mixture containing 20 mM MOPS, pH 7.0, 80 mM KCl, 5 mM $MgCl_2$, 0.1 mg of SR protein/mL, and either 0.2 mM $CaCl_2$ or 1 mM EGTA. Although the measurements displayed in the figures were obtained in the absence of Ca^{2+} (1 mM EGTA), identical data were obtained in the presence of 0.2 mM $CaCl_2$ (no EGTA). Fluorescence emission was measured at 540 nm wavelength, with excitation at 420 nm wavelength. Temp: 22 °C. The experimental points are matched by a curve generated by a single site binding equation, as in $E{\cdot}$TNP-AMP $= K[E_{tot}][\text{TNP-AMP}]/1 + K[\text{TNP-AMP}]$, where $E = 1$, and $K = 1 \times 10^6$ M^{-1} for the control, and $K = 5 \times 10^5$ M^{-1} for DIDS derivatized enzyme.

TNP-AMP is negligibly fluorescent in aqueous solution, but it develops a fluorescent signal upon binding to the SR ATPase (*29*, *30*). We now find that, upon careful titration of ATPase at low concentrations, TNP-AMP binding occurs over the 0.1−10.0 μM of TNP-nucleotide concentration range, and the experimental data are matched satisfactorily by a curve generated with a single site binding equation, assuming a 1×10^6 M^{-1} binding constant (Figure 8). The fluorescence titration curve is the same in the presence and

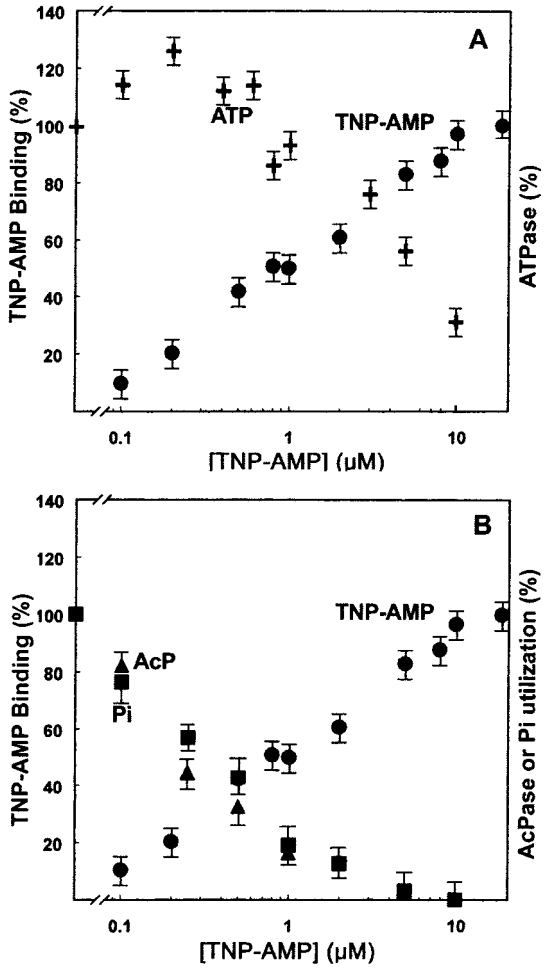

FIGURE 9: TNP-AMP binding (●), and its effect on ATPase (+) and AcPase (▲) activities, and on enzyme phosphorylation by Pi (■). ATPase and AcPase activities were measured in the presence of 20 mM MOPS, pH 7, 80 mM KCl, 5 mM Mg Cl_2, 0.2 mM $CaCl_2$, 3 or 50 μg of SR protein/mL, and 3 mM ATP or 4 mM AcP. Enzyme phosphorylation with Pi (50 μM) was measured (in the absence of Ca^{2+}) as described for Figure 4. TNP-AMP concentrations were as indicated in the figure. Binding and functional effects are expressed in percentage of maximal binding or function. Note that the ATPase activity is increased by low TNP-AMP concentrations but inhibited by higher TNP-AMP concentrations.

in the absence of Ca^{2+}, indicating that TNP-AMP binding occurs independently of whether the enzyme is in the Ca^{2+} bound (E_1) or the Ca^{2+} free (E_2) conformation.

TNP-AMP binding occurs (in the presence and in the absence of Ca^{2+}) even when Lys492 and Lys515 are cross-linked with DIDS. The TNP-AMP concentration dependence of binding, however, is significantly displaced as a consequence of derivatization (Figure 8), suggesting a reduction in binding affinity by the presence of DIDS label near the bound nucleotide. Furthermore, enzyme derivatization with DIDS appears to influence the fluorescence of bound TNP-AMP, as the fluorescence intensity upon maximal binding is reduced significantly likely due to a different environment in the derivatized enzyme (Figure 8). Considering the perturbation of the adenosine pocket introduced by lysine derivatization, the occurrence of TNP-AMP binding (albeit with lower affinity) indicates that interactions of the TNP moiety with the enzyme provide additional stabilization to the analogue, as compared with ATP.

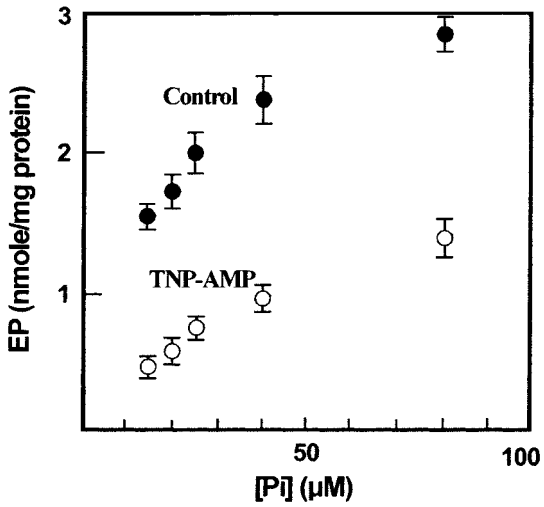

FIGURE 10: Pi concentration dependence of enzyme phosphorylation in the absence and in the presence of TNP-AMP. Enzyme phosporylation with Pi was obtained as described for Figure 4, in the absence of Ca^{2+}. The Pi concentration was changed as indicated. The TNP-AMP concentration was 2 μM. Phosphoenzyme (EP) is given in nmol/mg of protein.

Having defined the TNP-AMP binding characteristics, we then investigated the effect of TNP-AMP on utilization of ATP, AcP, or Pi by the enzyme. As previously noted (*31*), we observed that, in the presence of millimolar ATP, very low concentrations of TNP-AMP (0.1−0.5 μM) actually increase ATPase activity, but higher concentrations (1−10.0 μM) produce a progressive inhibition (Figure 9A). Inhibition of AcP utilization is also produced by TNP-AMP (Figure 9B), within a slightly lower concentration range, and without the activating effect of low concentrations. Interestingly, TNP-AMP inhibits also enzyme phosporylation by Pi in the absence of Ca^{2+} (Figures 9B and 10), even though this reaction occurs at the phosphorylation site (P domain), with no requirement for occupancy of the nucleotide and Ca^{2+} sites.

Effects of DIDS or TNP-AMP on Orthovanadate Dependent Photocleavage of the ATPase, and Orthovanadate Protection of ATPase Digestion with Proteinase K. Orthovanadate has been widely used to form a transition state analogue of the phosphorylation reaction in the SR ATPase (*13*, *32*, *33*). Its presence at the phosphorylation site (i.e., Asp351) can be demonstrated by photoactivated cleavage of the enzyme in correspondence of Thr353 (*34*). Cleavage occurs optimally in the presence of Ca^{2+} and ADP, consistent with formation of a transition state analogue of the phosphorylation reaction. We now find that the presence of DIDS or TNP-AMP in the adenosine binding pocket does not substitute for ADP in enhancing orthovanadate dependent photocleavage (Figure 11A). In fact, DIDS and TNP-AMP prevent even the photocleavage obtained with orthovanadate in the absence of ADP (Figure 11A).

Further information on the conformation of extramembranous (i.e., cytosolic) domains, can be derived from the pattern of ATPase digestion with proteinase K *(35−37)*. We found that, in the absence of Ca^{2+}, orthovanadate protects the ATPase from digestion with proteinase K. Protection, as revealed by the intensity of the 100-kD ATPase band and the presence of digestion product, is not observed when the ATPase is cross-linked with DIDS (Figure 11B). This

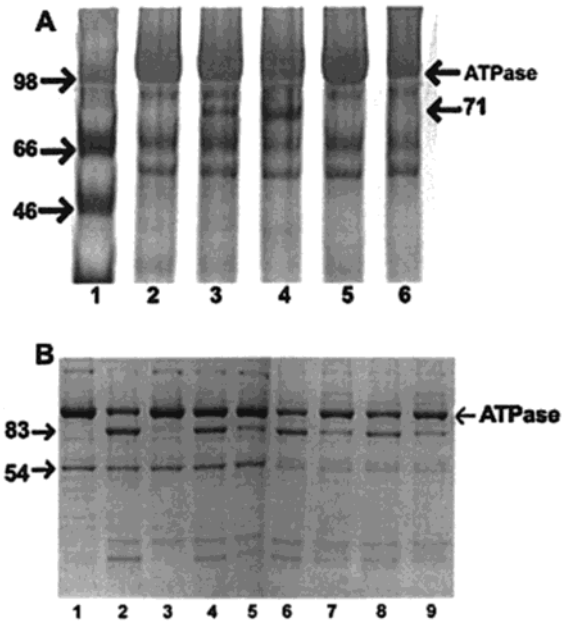

FIGURE 11: Effect of DIDS or TNP-AMP on orthovanadate dependent photocleavage of Ca^{2+} ATPase (A), and on orthovanadate protection of ATPase digestion by proteinase K (B). (A) Photooxidation was carried out with a reaction mixture containing 1 mg of SR protein/mL (control or cross-linked with DIDS), 50 mM Tris-HCl buffer, pH 8.6 (to avoid formation of decavanadate), 100 mM KCl, and 5 mM $MgCl_2$, in the absence or in the presence of 1 mM orthovanadate and/or 1 mM ADP. Following 30 min preincubation, the reaction mixture was illuminated for 15 min with long wavelength UV light, and the protein was subjected to electrophoretic analysis. The 71-kD band is generated by cleavage in correspondence of Thr353. 1: molecular weight standards; 2: photocleavage control; 3: photocleavage with orthovanadate; 4: photocleavage with orthovanadate and ADP; 5: photocleavage with orthovanadate in the presence of TNP-AMP; and 6: photocleavage with orthovanadate following cross-linking with DIDS. (B) Limited digestion with proteinase K was carried out with a reaction mixture containing 0.3 mg of SR protein (control or cross-linked with DIDS)/mL, 50 mM MOPS buffer, pH 8.0, 50 mM NaCl, 5 mM $MgCl_2$, 2 mM EGTA, in the absence or in the presence of 1 mM orthovanadate and/or 1 mM ADP. Following 30 min preincubation, the mixture was incubated with 0.01 mg/mL proteinase K at 25 °C for 40 min, and quenched by addition of ice-cold trichloroacetic acid to 2.5% (w/v). The protein was then subjected to electrophoretic analysis. 1: control ATPase; 2: control ATPase digested; 3: control ATPase digested in the presence of orthovanadate; 4: control ATPase digested in the presence of ADP; 5: control ATPase digested in the presence of orthovanadate and ADP. 6, 7, 8, and 9: the same sequence (as 2, 3, 4, and 5) was repeated following ATPase cross-linking with DIDS. In panel B, the efficiency of digestion is best evaluated by comparing residual densities of the ATPase bands. The numbers referred to electrophoretic bands by arrows, define their MW in kDa.

suggests that structural perturbation of the adenosine binding pocket within the N domain, interferes with vanadate binding at the phosphorylation site. These experiments were performed in the absence of Ca^{2+}, to minimize protection by ADP, which is Ca^{2+} dependent.

DISCUSSION

Structural definition of the pocket including the reactive residues Lys492 and Lys515 as well as the TNP-AMP binding site provides a very useful guide for experimental perturbations of the N-domain, and evaluation of its role in the catalytic and transport cycle. In fact, conditions were already established for derivatization of Lys492 with PYP

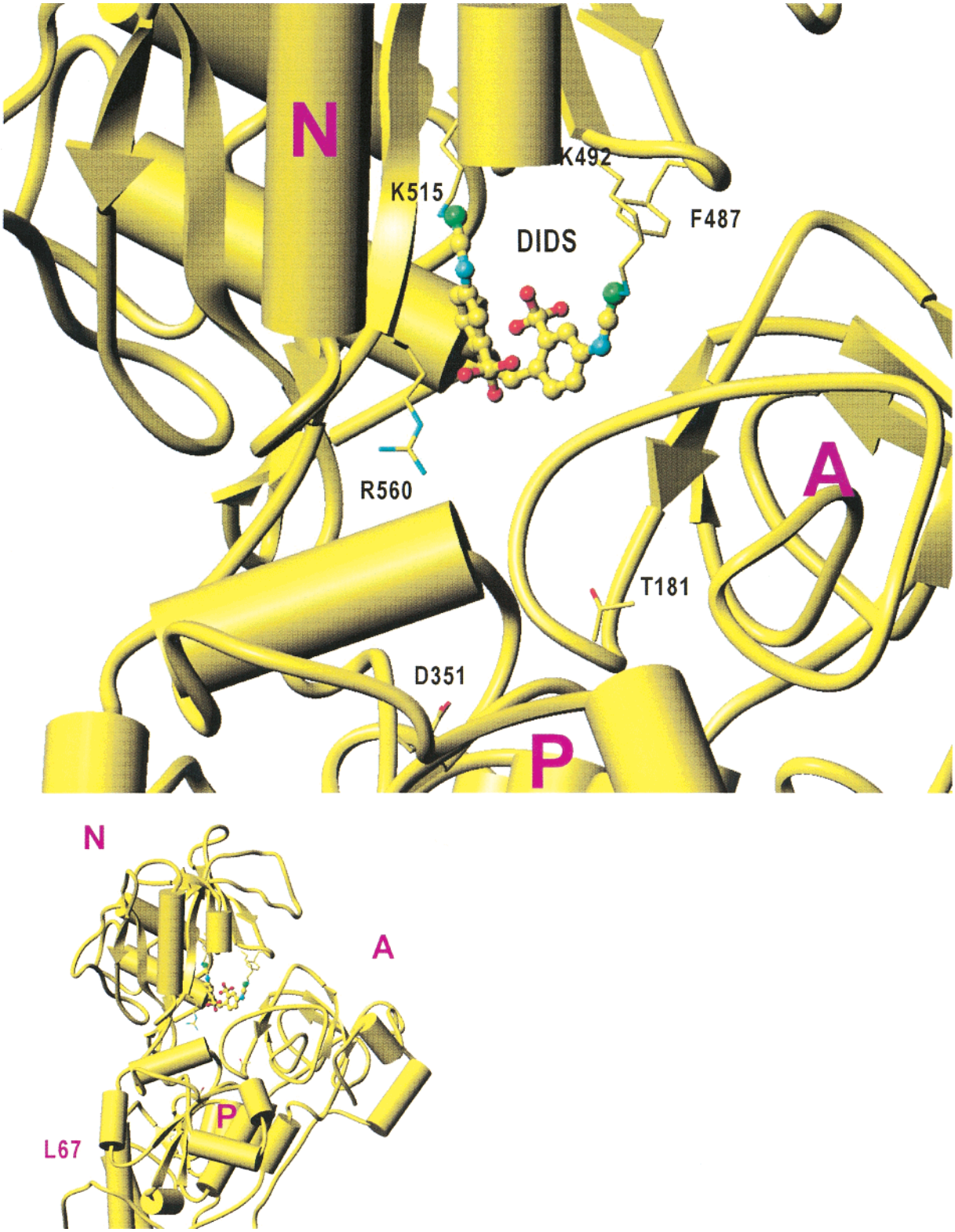

FIGURE 12: Three-dimensional structure of the Ca^{2+} ATPase around the adenosine binding pocket of the N domain, and neighboring P and A domain. The geometry of DIDS cross-linking was derived by modeling energy minimized DIDS coordinates in the E_2P analogue of the Ca^{2+} ATPase. The analogue structure is based on the theoretical model deposited on PBD (accession code 1FQU). The smaller image represents the relative positions of the N, P, and A domains, while the larger figure shows the positions of relevant residues. Asp351, in the P domain, is the residue undergoing intermediate phosphorylation. Note the proximity of Arg560 to the DIDS label and to Asp351.

(*8*, *9*), derivatization of Lys515 with FITC (*6*, *7*), and cross-linking of Lys492 and Lys515 with DIDS (*10*). We find that selective derivatization of Lys492 with PYP, or Lys515 with FITC, produces total ATPase inhibition when ATP is the substrate (Figure 2), due to interference with ATP binding (*6*). Accordingly, only partial inhibition is observed when AcP is the substrate (Figure 3), and no inhibition at all when Pi is utilized for reverse formation of phosphorylated intermediate (Figure 4). Furthermore, coupling of AcP utilization with Ca^{2+} transport (*28*) is retained by the derivatized enzyme, indicating that functional linkage of phosphorylation and Ca^{2+} sites is still operative. These

experiments demonstrate that selective derivatization of Lys492 or Lys515 interferes specifically with binding and delivery of the ATP substrate to the catalytic site, but does not disrupt primarily the catalytic mechanism.

Cross-linking of Lys492 and Lys515 with DIDS, on the other hand, produces strong inhibition of all ATPase reactions, including ATP or AcP utilization in the presence of Ca^{2+} (Figures 2, 3, and 5), and reverse formation of phosphorylated intermediate by utilization of Pi in the absence of Ca^{2+} (Figure 4). This is an important result, indicating that the presence of DIDS in the N domain interferes with phosphorylation reactions at the catalytic site, independent of whether the substrate is a nucleotide or not, and of the presence or the absence of Ca^{2+}. It is then apparent that the presence of the DIDS cross-linking does not allow proper interaction of N and P domain, and this interaction is required for ATPase functional integrity. It is shown in Figure 12 that cross-linking Lys492 and Lys515 with DIDS effectively closes the nucleotide binding pocket and presumably interferes with proper interfacing of complementary protein segments.

Further insight may be gained considering the close proximity of Arg560 to DIDS or TNP-AMP (TNP moiety). This proximity is revealed by the geometries of TNP-AMP binding (derived from difference Fourier synthesis of ATPase three-dimensional crystal soaked in TNP-AMP solutions (*1*)) and of DIDS cross-linking (derived by modeling energy minimized DIDS coordinates (Figure 12)). It is most interesting that single mutation of Arg560 produces strong inhibition of ATPase activity and phosphoenzyme formation by utilization of ATP (Figure 11A), indicating that Arg560 plays an important role in stabilizing the nucleotide substrate. It is important to compare, in this regard, the inhibitory effect of Arg560 mutation, with the lack of inhibitory effects by Lys 492 or Lys515 mutations (*38*). This indicates that the inhibitory effect of Lys 492 and Lys515 derivatization is actually due to steric hindrance by the PYP and FITC labels. On the other hand, the inhibition produced by the Arg 560 mutation is evidently due to interference with a direct role of Arg 560 in stabilization of the nucleotide substrate.

Another approach to probing the Lys492/Lys515 pocket is based on the use of TNP-AMP. It was previously reported that TNP derivatives of adenosine nucleotides bind to the SR ATPase with a 1:1 stoichiometry (*29*). In fact, Lys492 can be derivatized with 8- (*31*) or 2-azido-TNP-AMP (*39*). Furthermore, the presence of TNP-AMP within the Lys492/Lys515 pocket has been demonstrated by crystallographic analysis of the enzyme in the presence of Ca^{2+} (*1*). Our experiments showing that TNP-AMP binding is retained, although with reduced affinity, by the Lys492/Lys515 derivatized enzyme, suggest that the TNP moiety confers additional stabilization to the bound analogue, as compared with ATP. It is conceivable that TNP-AMP binds to the enzyme at a (virtually) identical site as ATP, but with altered geometry. This idea is consistent with the model of TNP-AMP bound to the enzyme derived from crystallographic analysis (i.e., miss-oriented phosphate moiety). The model also reveals the proximity of Arg560, suggesting that its positive charge may provide stability by interaction with NO_2 in the TNP moiety.

The inhibition of substrate utilization produced by TNP-AMP or DIDS, indicate that experimental perturbations of the N domain interfere with catalytic events occurring in the P domain. Presumably, TNP-AMP and DIDS provide obstacles to substrate occupancy of the phosphorylation site. In fact, orthovanadate dependent photocleavage, and orthovanadate protection of ATPase from digestion with proteinase K, are prevented by Lys492/Lys525 derivatization with DIDS or by the presence of TNP-AMP (Figure 11). Therefore, these perturbations of the N domain interfere even with formation of the phosphorylation transition state analogue by orthovanadate. It is then apparent that appropriate closure of N, P, and A domains occurs in concomitance with substrate utilization (*37*), as enzyme phosphorylation is likely to be favored by hydrophobic effects produced by the closure. In fact, phosphoryl transfer reactions are strongly dependent on water activity and the characteristics of the local environment (*40*). Proper closure of such domains is evidently interfered with by our experimental perturbations.

An additional point of interest is related to the observation that, while relatively high concentrations (1−10 μM) of TNP-AMP are inhibitory, low concentrations (0.1−0.3 μM) of TNP-AMP stimulate ATPase activity (Figure 8; *32*, *41*). It is likely that, given a favorable concentration ratio of TNP-AMP and ATP, TNP-AMP can bind transiently in exchange for dissociating ADP upon transfer of the ATP terminal phosphate to the enzyme, thereby producing an activating effect (*42*−*44*). This is an effect that is also produced by ATP itself, as the ATPase dependence on ATP concentration includes a first rise due to occupancy of the substrate site with high affinity, and a second rise due to occupancy of the activating site with lower affinity (Figure 2). It is likely that the ATP substrate is bound with its adenosine moiety in the N domain and is stabilized further by interactions of its gamma-phosphate moiety within the P domain with Mg^{2+} participation. Following phosphoryl transfer, the N domain would then relax, dissociate ADP, and allow binding of activating ATP (or TNP-AMP) with lower affinity. Measurements of Pi ↔ HOH exchange (*42*) indicate that the activating effect of high ATP is related to an increase of the phosphoenzyme level available to medium water. We consider that low affinity nucleotide binding to the phosphorylated enzyme (following ADP dissociation) may occur by interaction of its adenosine moiety with the Lys492/Lys515 pocket, but lacking stabilization of its gamma-phosphate within the P domain. This would favor dissociation of the cytoplasmic domains, thereby rendering the phosphorylation site more exposed to medium water and favoring hydrolytic cleavage of Pi.

REFERENCES

1. Toyoshima, C., Nakasako, M., Nomura, H., and Ogawa, H. (2000) *Nature 405*, 647−655.
2. Toyoshima, C., Sasabe, H., and Stokes, D. L. (1993) *Nature 362*, 469−471.
3. Zhang, P., Toyoshima, C., Yonekura, K., Green, N. M., and Stokes, D. L. (1998) *Nature 392*, 835−839.
4. Clarke, D. M., Loo, T. W., Inesi, G., and MacLennan, D. H. (1989) *Nature 339*, 476−478.
5. Stokes, D. L., and Green, N. M. (1990) *Biophys. J. 57*, 1−14.
6. Pick, U., and Bassilian, S. (1981) *FEBS Lett. 123*, 127−136.
7. Mitchinson, C., Wilderspin, A., Trinnaman, B. J., and Green, N. M. (1982) *FEBS Lett. 146*, 87−92.
8. Murphy, A. J. (1977) *Arch. Biochem. Biophys. 180*, 114−120.

9. Yamagata, K., Daiho, T., and Kanazawa, T. (1993) *J. Biol. Chem. 268*, 20930−20936.
10. Hua, S., and Inesi, G. (1997) *Biochemistry 36*, 11865−11872.
11. Gatto, C., Lutsenko, S., and Kaplan, J. H. (1997) *Arch. Biochem. Biophys. 340*, 90−100.
12. Eletr, S., and Inesi, G. (1972) *Biochim. Biophys. Acta 282*, 174−179.
13. Pick, U. (1981) *Eur. J. Biochem. 121*, 187−195.
14. Zhang, Z., Lewis, D., Strock, C., Inesi., G., Nakasako, M., Nomura, H., and Toyposhima, C. (2000) *Biochemistry* 39, 8758−8767.
15. Lanzetta, P. A., Alvarez, L. J., Reinsch, P. S., and Candia, O. A. (1979) *Anal. Biochem. 100*, 95−97.
16. Lippman, F., and Tuttle, L. C. (1945) *J. Biol. Chem. 159*, 21−28.
17. Weber, K., and Osborn, M. (1969) *J. Biol. Chem. 244*, 4406−4417.
18. Laemmli, U. K. (1970) *Nature 227*, 680−685.
19. Inesi, G., Goodman, J. J., and Watanabe, T. (1967) *J. Biol. Chem. 242*, 4637−4643.
20. Pedemonte, C. H., and Kaplan, J. H. (1988) *Biochemistry* 27, 7966−7973.
21. Zhang, Z., Sumbilla, C., Lewis, D., Summers, S., Klein, M. G., and Inesi, G. (1995) *J. Biol. Chem. 270*, 16283−16290.
22. Masuda, H., and deMeis, L. (1973) *Biochemistry 12*, 4581−4585.
23. Kanazawa, T., and Boyer, P. D. (1973) *J. Biol. Chem. 248*, 3163−3172.
24. de Meis, L. (1969) *Biochim. Biophys. Acta 172*, 343−344.
25. Friedman, Z., and Makinose, M. (1970) *FEBS Lett. 11*, 69−72.
26. Pucell, A., and Martonosi, A. (1971) *J. Biol. Chem. 246*, 3389−3397.
27. Bodley, A., and Jencks, W. P. (1987) *J. Biol. Chem. 262*, 13997−14004.
28. Teruel, J. A., and Inesi, G. (1988) *Biochemistry 27*, 5885−5890.
29. Watanabe, T., and Inesi, G. (1982) *Biochemistry 21*, 3254−3259.
30. Nakamoto, R. K., and Inesi, G. (1984) *J. Biol. Chem. 259*, 2961−2970.
31. Seebregts, C. J., and McIntosh, D. B. (1989) *J. Biol. Chem. 264*, 2043−2052.
32. Dupont, Y., Pougeois, R., Ronjat, M., and Verjovski-Almeida, S. (1985) *J. Biol. Chem. 260*, 7241−7249.
33. Inesi, G., Kurzmack, M., Nakamoto, R., deMeis, L., and Bernhard, S. (1980) *J. Biol. Chem. 255*, 6040−6043
34. Hua, S., Inesi, G., and Toyoshima, C. (2000) *J. Biol. Chem. 275*, 30546−30550.
35. Juul, B., Turc, H., Durand, M. L., Gomez de Gracia, A., Denoroy, L., Moller, J. V., Champeil, P., and Le Maire, M. (1995) *J. Biol. Chem. 270*, 20123−20134.
36. Champeil, P., Menguy, T., Soulié, S., Juul, B., De Gracia, A. G., Rusconi, F., Falson, P., Denoroy, L., Henao, F., Le Maire, M., and Moller, J. V. (1998) *J. Biol. Chem. 273*, 6619−6631.
37. Danko, S., Daiho, T., Yamasaki, K., Kamidochi, M., Suzuki, H., and Toyoshima, C. (2001) *FEBS Lett. 489*, 277−282.
38. Andersen, P., and Vilsen, B. (1995) *FEBS Lett. 359*, 101−106.
39. Inesi, G., Cantilina, T., Yu, X., Nikic, D., Sagara, Y., and Kirtley, M. E. (1992) *Ann. NY Acad. Sci. 671*, 32−49.
40. deMeis, L., and Inesi, G. (1982) *J. Biol. Chem. 257*, 1289−1294.
41. Champeil, P., Riollet, S., Orlowski, S., Guillain, F., Seebregts, C. J., and McIntosh, D. B. (1988) *J. Biol. Chem. 263*, 12288−12294.
42. McIntosh, D. B., and Boyer, P. D. (1983) *Biochemistry 22*, 2867−2875.
43. Gould, G. W., East, J. M., Froud, R. J., McWhirter, J. M., Stefanova, H. I., and Lee, A. G. (1986) *Biochem. J. 237*, 217−227.
44. Bishop, J. E., Al-Shawi, M. K., and Inesi, G. (1987) *J. Biol. Chem. 262*, 4658−4663.

BI015684H